Carbothermal reduction vapor phase transport growth of ZnO nanostructures: Effects of various carbon sources

M. Biswas, E. McGlynn', M. O. Henry, M. McCann, and A. Rafferty

Citation: Journal of Applied Physics **105**, 094306 (2009); doi: 10.1063/1.3121213
View online: http://dx.doi.org/10.1063/1.3121213
View Table of Contents: http://aip.scitation.org/toc/jap/105/9
Published by the American Institute of Physics

Carbothermal reduction vapor phase transport growth of ZnO nanostructures: Effects of various carbon sources

M. Biswas,[1] E. McGlynn,[1,a)] M. O. Henry,[1] M. McCann,[2] and A. Rafferty[3]
[1]*School of Physical Sciences/National Centre for Plasma Science and Technology, Dublin City University, Glasnevin, Dublin 9, Ireland*
[2]*School of Chemical Engineering, University College Dublin, Dublin 4, Ireland*
[3]*School of Mechanical and Manufacturing Engineering, Dublin City University, Glasnevin, Dublin 9, Ireland*

(Received 2 March 2009; accepted 20 March 2009; published online 4 May 2009)

ZnO nanostructures were grown via carbothermal reduction vapor phase transport with carbon black, activated carbon, and graphite powders. Nanostructures can be grown at significantly lower temperatures with carbon black and activated carbon, although with different morphologies compared to graphite. The surface areas of the carbon black and activated carbon are higher than those of graphite; this has been used previously to explain the origin of such growth and morphology differences. We use different ZnO/graphite ratios to equalize surface areas compared to carbon black and eliminate this effect, but differences in nanostructure growth and morphology remain. We discuss the effects of thermodynamics and carbon purity and conclude that the high surface activities of the carbon black and activated carbon are the reason for our results. © *2009 American Institute of Physics*. [DOI: 10.1063/1.3121213]

INTRODUCTION

ZnO nanostructures grown using the relatively simple method of vapor phase transport (VPT) have shown a wide variety of morphologies with very good crystalline quality and optoelectronic properties.[1–4] A very common Zn vapor source in VPT growth of ZnO nanostructures is a mixture of carbon and ZnO powders whereby carbon is used as a reducing agent to produce Zn vapor.[3,4] The mechanism, known as carbothermal reduction (CTR), is popular as it allows control of the Zn vapor pressure via the reaction temperature.[5,6] CTR-VPT growth of ZnO nanostructures is usually done at temperatures $>900\ ^{\circ}C$. The ability to grow ZnO nanostructures at lower temperatures is desirable as it would broaden the range of possible substrates and also reduce undesirable high temperature effects such as unwanted dopant diffusion from substrate to nanorods (e.g., Al from sapphire substrates[7]) and substrate-nanorod reactions.[8] It has been observed experimentally that the use of other types of carbon such as carbon black, single walled nanotubes (SWNT), multiwalled nanotubes (MWNT), and activated carbon can all be used to grow ZnO nanostructures at lower temperatures.[8–11] Interestingly, at certain temperatures, no growth at all was found using graphite, whereas nanostructures were grown using these other carbon sources.[8,9] This was explained by previous authors in terms of the higher total surface area (TSA) of nongraphite carbon sources (such as those mentioned above) leading to an increase in released Zn vapor responsible for nanostructure growth,[8] and by others as due to the effects of lower purity in the carbon source.[9] In a previous work we have questioned the former explanation and commented that as well as surface area one must also consider factors such as differences in free energy of carbon sources and effects on the reaction energetics.[12] Additionally, the surface activity of nongraphite carbon sources (originating in edges and defects of the carbon layers and the presence of heteroatoms such as oxygen, hydrogen, sulfur, and nitrogen which introduce active sites on the carbon surface) is known to play a considerable role in the surface chemistry of the material.[13] The surface activity is related to the surface area (and is expected to scale with surface area for otherwise identical materials) but is not correlated solely with changes in the surface area, and the density of active sites is strongly dependent on material preparation methods. Hence, different carbon materials with identical surface areas can have different surface activities due to differences in preparation.[13] Finally, the available purity levels of these nongraphite carbon sources is often, or even generally, inferior to the available purity levels in graphite, and impurities can affect nanostructure growth, e.g., indium (In) impurity contamination of the growth system is known to significantly alter the growth morphology and alignment of ZnO nanostructures in CTR-VPT growth.[14] The need to ensure reproducibility and control of nanostructure morphology is in general an even more important consideration than unwanted high temperature effects. Hence, the appropriate selection of the carbon source is an important factor and the relative effects of carbon source surface area, surface activity, thermodynamic stability, and purity remain unclear.

In this paper, we present CTR-VPT growth of ZnO nanostructures at different temperatures using carbon black, activated carbon, and graphite powders. We have directly compared the observed ZnO deposit where identical total carbon surface areas for graphite and carbon black were used to test the previously reported hypothesis of a kinetic limitation on growth due to surface area. We have also studied the effects of using very high surface area activated carbon,

a)Author to whom correspondence should be addressed. Electronic mail: enda.mcglynn@dcu.ie.

compared both to carbon black and graphite. The ZnO deposits grown using carbon black and activated carbon are similar and differ significantly in quantity and morphology from those grown with graphite. We find that ZnO nanostructures grow at 750 °C using carbon black and activated carbon, but no growth is seen at this temperature when using graphite even where identical TSAs compared to carbon black are used. We discuss these data and comment on the effect on the Ellingham diagram of differences in Gibb's energy of different carbon powders, in addition to differences in impurity levels. We conclude that these differences are largely insignificant and that the high surface activity of activated carbon and carbon black sources compared to graphite is the likely explanation of our data.

EXPERIMENTAL PROCEDURE

ZnO nanostructures were grown using the CTR-VPT method on the *a*-plane $(11\bar{2}0)$ sapphire using the vapor-liquid-solid mechanism. An Au film with nominal thickness of 5 nm was used as the catalyst. An Ar carrier gas flow of 90 SCCM (SCCM denotes cubic centimeters per minute at STP) was used. The sample was placed on either an alumina or quartz boat, directly above the source powder (ensuring identical source and sample temperatures), in the middle of the single zone furnace, and growth was carried out at atmospheric pressure for a time period of 60 min. Zn vapors were produced by CTR of high purity ZnO powder (Alfa Aesar; 99.9995%). Three types of carbon source were used: (a) graphite (Alfa Aesar; 99.9999% purity), (b) carbon black (Micromeritics: 99% purity—a partially graphitizing carbon), and (c) activated carbon (Sigma-Aldrich; untreated activated carbon, 99% purity—a nongraphitizing carbon). The specific surface area (SSA) of these three types of powder was measured using the Braunauer–Emmett–Teller (BET) method. Adsorption isotherms using nitrogen were obtained for each of the powders using a Nova 2200® surface area analyzer (Quantachrome Instruments). The SSA is the TSA per unit mass and, for porous solids, may be attributed predominantly to the total internal surface area of open pores. The ZnO and carbon source powders were well mixed using mortar and pestle before CTR-VPT. SSA measurements before and after this mechanical procedure indicate that the mixing process does not affect the SSA of either species. Our "normal" procedure uses ZnO powder and carbon powder masses of 0.06 g each (1:1 mass ratio giving a molar excess of C). In some experiments we equalized the total carbon surface area between growths with carbon black and graphite by varying the relative mass of graphite powder to ZnO powder. Therefore, since the SSA of graphite powder used is lower than that of carbon black, in these experiments we used a larger mass of graphite to equalize the surface areas. The relative difference in SSA between graphite and carbon black was such that this could be done while maintaining the growth chamber physical configuration in a nearly identical fashion; however, the relative difference in SSA between graphite and activated carbon was too large for this procedure to be used, as a very large graphite mass would have been required, leading to a significant alteration of the growth chamber physical configuration. Samples were characterized by high resolution field emission scanning electron microscopy (FESEM) (Hitachi S-4300 field emission system or Tescan Mira II field emission system) and x-ray diffraction (XRD) (Bruker AXS D8 advance texture diffractometer).

TABLE I. SSA values for the various carbon source powders used in the CTR process and the ZnO powder used.

Powder	SSA (m^2/g)
Graphite	2.6
Carbon black	28.5
Activated carbon	1000
ZnO	7.9

RESULTS AND DISCUSSION

We begin by noting the details of the reactions that govern CTR-VPT growth for the ZnO nanostructures under consideration here.[6] These reactions are as follows:

$$\mathrm{ZnO}(s) + \mathrm{C}(s) \rightarrow \mathrm{Zn}(g) + \mathrm{CO}(g), \quad (1)$$

$$\mathrm{ZnO}(s) + \mathrm{CO}(g) \rightarrow \mathrm{Zn}(g) + \mathrm{CO_2}(g), \quad (2)$$

$$\mathrm{CO_2}(g) + \mathrm{C}(s) \rightarrow 2\mathrm{CO}(g). \quad (3)$$

At the normal range of growth temperatures (>700 °C), the gases produced by reaction (1) are $\mathrm{Zn}(g)$ and $\mathrm{CO}(g)$, although at lower temperatures $\mathrm{CO_2}$ may also be produced even for molar equalities or excesses of C.[6] The overall reaction (at high temperatures) is given by Eq. (1), and it is known that this proceeds by two intermediate reactions shown in Eqs. (2) and (3), so the actual reaction pathway is via solid-gas reactions, and thus may be sensitive to the solid surface area. Previous work has established that the step contained in Eq. (3) (the producer gas reaction) is the slower one and thus carbon surface area and activity may be the key factors in CTR-VPT growth of ZnO nanostructures.[6] For this reason, we have examined the effects of changes in the carbon surface area only and kept the ZnO powder surface area constant.

The BET calculated SSA results are presented in Table I. For reference, the ZnO powder surface area is constant in all experiments. Since the carbon black SSA is 10.9 times higher than that of graphite, for certain experiments [samples shown in Figs. 3(a)–3(c)] a graphite weight of 10.9 $\times$0.06 g (=0.654 g) was used (keeping the amount of ZnO powder identical, i.e., 0.06 g), yielding an equivalent carbon surface area (1.7 m^2) for both graphite and carbon black powders. Since there remains a molar excess of C, the thermodynamics of reactions (1)–(3) are not affected.[6] This allowed a direct comparison of the effect of the kinetics due to the surface area.

Figure 1 shows the scanning electron micrograph (SEM) of the samples in the Au-deposited region for CTR-VPT growth using graphite and carbon black at different temperatures with the normal mass of carbon (0.06 g). The left col-

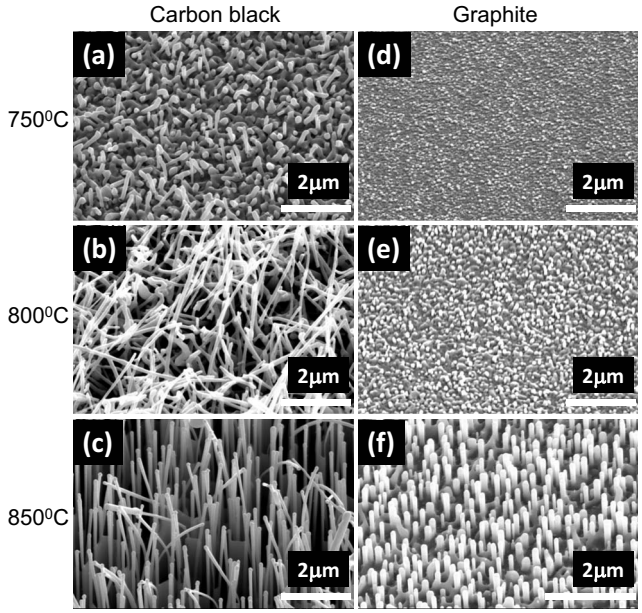

FIG. 1. FESEM images of samples grown using carbon black at (a) 750 °C, (b) 800 °C, and (c) 850 °C and using graphite at (d) 750 °C, (e) 800 °C, and (f) 850 °C (using a carbon powder mass of 0.06 g in both cases).

umn images (a), (b), and (c) correspond to ZnO nanostructures grown using carbon black and the right column images (d), (e), and (f) correspond to ZnO nanostructures grown using graphite (750 °C [(a) and (d)], 800 °C [(b) and (e)], and 850 °C [(c) and (f)]). Further experiments were carried out in the temperature range of 700–950 °C for both types of powder. Differences in growth and morphology can be observed in these images for the two different carbon source powders, which is especially visible for growths at 750 and 800 °C, although the morphology for growth at 850 °C is also quite different, with substantially longer, generally narrower, higher density, and less well-aligned nanostructures being grown using carbon black compared to graphite. Figure 2 shows the 2θ-ω XRD data of the same samples. The left columns again show data for samples grown using carbon black and the right column are for samples grown using graphite (750 °C [(a) and (d)], 800 °C [(b) and (e)], and 850 °C [(c) and (f)]). All samples show the Al_2O_3 $(11\bar{2}0)$ peak at 37.78° due to the sapphire substrate. Peaks corresponding to ZnO are seen in all samples, except that grown using graphite at 750 °C, where the ZnO peaks are below the detection limit. No XRD peaks corresponding to other phases are seen.[15] For samples grown with carbon black the ZnO (0002) peak at 34.42° and ZnO $(10\bar{1}1)$ peak at 36.25° are seen in all samples, consistent with the unaligned growth of ZnO nanostructures seen in Figs. 1(a)–1(c). For samples grown with graphite, the (0002) peak is seen as the dominant peak in Figs. 2(e) and 2(f), consistent with the *c*-axis aligned growth seen in Figs. 1(e) and 1(f)—although some slight evidence of the $(10\bar{1}1)$ peak is also seen due to unaligned crystallites. The fact that no ZnO peaks are observed above the detection limit of the instrument in Fig. 2(d) is consistent with the absence (or very small quantity) of the observed ZnO growth in Fig. 1(d). The higher order ZnO (0004)

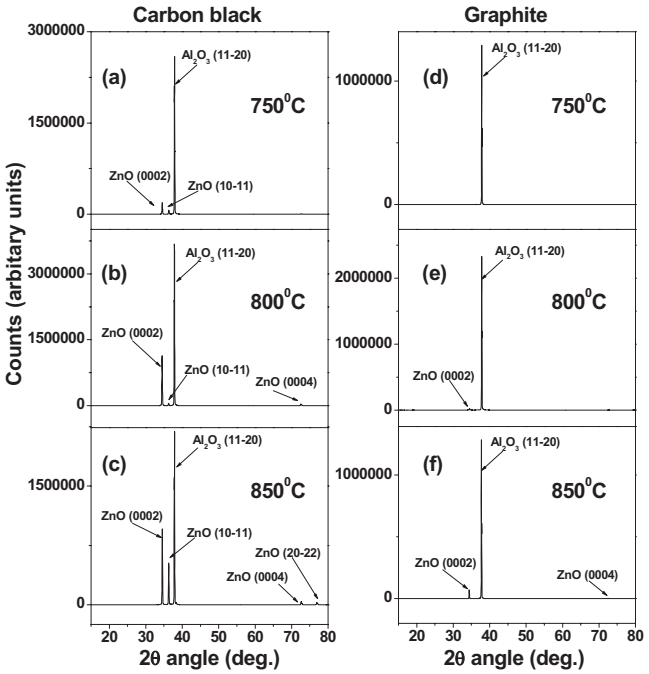

FIG. 2. 2θ-ω XRD data of the samples grown using carbon black at (a) 750 °C, (b) 800 °C, and (c) 850 °C and using graphite at (d) 750 °C, (e) 800 °C, and (f) 850 °C (using a carbon powder mass of 0.06 g in both cases).

(72.50°) peak is seen in Figs. 2(b), 2(c), and 2(f), while the ZnO $(20\bar{2}2)$ peak (76.90°) is seen in Fig. 2(c) only.

Figure 3 shows SEM images of samples grown using graphite with different TSAs from 750 to 850 °C. As stated above, we varied the TSA by varying the weight of the graphite powder keeping all other conditions identical. The high TSA (HTSA) sample in Figs. 3(a)–3(c) had a carbon TSA of 1.7 m^2 [the same TSA as the carbon black used to grow the samples shown in the Figs. 1(a)–1(c)] and the low

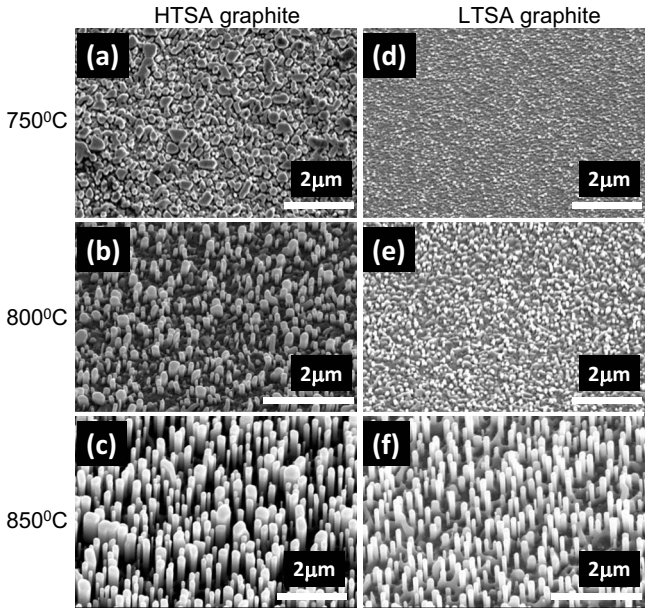

FIG. 3. FESEM images of samples grown using HTSA graphite (mass =0.654 g) at (a) 750 °C, (b) 800 °C, and (c) 850 °C and using LTSA graphite (mass=0.06 g) at (d) 750 °C, (e) 800 °C, and (f) 850 °C.

TSA (LTSA) sample in Figs. 3(d)–3(f) had a carbon TSA of 0.156 m^2 [mentioned above as the normal procedure, and identical to the samples in Figs. 1(d)–1(f)]. However, it is clear that the ZnO morphology and deposit quantity are very similar for both samples. There is a slightly greater volume of deposit for the HTSA sample at all temperatures—the nanorod density determined from the SEM data for the LTSA sample at 850 °C is slightly >80% of the density for the HTSA sample at the same temperature, and the LTSA nanorods are slightly shorter and narrower than the HTSA nanorods.

The data shown above in Fig. 1 (and supported by Fig. 2) clearly demonstrate that the ZnO nanostructures grown with carbon black have a very different yield and morphology to those grown with LTSA graphite, with, e.g., large deposits of partially aligned and thin nanowires (diameters of ~50 nm and lengths of ~10 μm) grown using carbon black at 850 °C, while well-aligned nanorods (diameters of ~150 nm and lengths of <5 μm) are seen for growth using LTSA graphite at 850 °C. In addition, while substantial ZnO deposits are seen using carbon black at 750 and 800 °C, almost no deposit is seen at 750 °C (some nucleation is seen) and only the beginnings of nanorod nucleation are seen for growth using LTSA graphite at 800 °C. Further SEM and XRD results (not shown) indicate no observable growth is found at or below 700 °C for carbon black powder. When we equalized the total graphite surface area to that of the carbon black (HTSA), as shown in Fig. 3, the growth morphology is very similar to that obtained using LTSA graphite. The reduced carbon surface area associated with the LTSA sample results in an almost negligible reduction in the quantity of nanostructure growth. Previous work has compared growth with different carbon powders on Si substrates where in all cases unaligned growth is observed due to the absence of epitaxial growth conditions.[8,9] The advantage of using *a*-sapphire substrates is that one can observe both clear changes in morphology from well aligned (using graphite, which is the normal situation due to the epitaxial growth of ZnO on sapphire) to poorly or unaligned (using carbon black or activated carbon) in addition to changes in yield. Our experiments thus have two methods for comparing changes in growth.[12]

The conclusion we draw is that while the carbon powder source type is of extreme importance in determining the yield and morphology of the ZnO deposit and enables growth at lower temperatures, the origin of this effect is not in the differing surface areas of different carbon source powders, as hypothesized previously.[8,16] There remain three possible sources of this effect; (i) differing free energies (which alter the Ellingham diagram[5]), (ii) differing levels of impurities, or (iii) differing surface activities for the different carbon powders.

We discuss the effects of different carbon powder free energies first. Carbon black is a (partially) graphitizing form of carbon, while activated carbon is nongraphitizing.[17,18] Graphite is the thermodynamically stable form of carbon, and the specific Gibbs free energies of other forms (including diamond and amorphous forms) are always larger than those of graphite.[19] The varying methods of production and the varying microstructure and chemical bonding of different carbons mean that a wide range of specific Gibbs free energies may be possible. In general the excess free energy for internal atoms (i.e., atoms not at edges and defects of the carbon layers or at locations where heteroatoms introduce active sites on the carbon layer surface) in turbostratic packing appropriate to carbon blacks (and other graphitizing forms of carbon) above the graphite value is ~3–5 kJ/mol in the temperature regime used in this study.[20,21] However, values of up to ~33 kJ/mol have been reported by other authors, for nongraphitizing forms, symptomatic of the varying microstructure, and chemical bonding referred to above and especially the very distinct and porous microstructure of nongraphitizing forms.[22] The likely effects of the changes in Gibbs free energy for the samples of the type shown in Fig. 1 using graphite and carbon black can be judged in terms of shifts in the critical temperatures on the Ellingham diagram. In terms of moles of O_2, the $2C+O_2 \rightarrow 2CO$ line on the Ellingham diagram shifts downward by ~6–10 kJ for CTR using carbon black.[20,21] This corresponds to a downward shift in the temperature where the $2Zn+O_2 \rightarrow 2ZnO$ line crosses the $2C+O_2 \rightarrow 2CO$ line of ~8–16 °C. We can say that the effect of the differing free energy of the carbon black is to allow the CTR reaction to proceed at temperatures about 20 °C lower than with graphite. This is clearly insufficient to explain our data in Fig. 1, where the differences in yield and morphology between growth using LTSA graphite at 800 °C and carbon black at 800 °C [Figs. 1(b) and 1(e)] are not comparable to the differences in growth using using LTSA graphite at 800 and 850 °C [Figs. 1(e) and 1(f); a 50 °C temperature difference]. Thus we conclude that the effects of differing Gibbs free energies between the graphite and carbon black powders cannot explain our data. These conclusions are valid also when comparing the differences in yield and morphology using HTSA graphite at 800 and 850 °C [Figs. 3(b) and 3(c)] to the difference in yield and morphology between growth using carbon black at 800 °C and HTSA graphite at 800 °C [Figs. 1(b) and 3(b)].

The conclusions that neither carbon source surface area nor thermodynamic stability explain our data are supported by the data for growth with the normal carbon weight (0.06 g) using activated carbon (a nongraphitizing carbon with a high surface area of 1000 m^2/g) shown in Figs. 4(a)–4(c) for growth at various temperatures [Fig. 4(a)—750 °C; Fig. 4(b)—800 °C; and Fig. 4(c)—850 °C]. The growths are quite similar both in terms of quantity and morphology of the deposit to those found using carbon black at similar temperatures [shown for comparison in Figs. 4(d)–4(f) and identical to the samples in Figs. 1(a)–1(c)]. This is despite the fact that (i) the activated carbon as a much (~30 times) higher SSA than carbon black and (ii) that it is nongraphitizing carbon whose Gibbs free energy is probably larger than that of carbon black and thus likely to push the critical CTR reaction temperatures to even lower values.

Another possible factor to explain the results we see is the carbon purity. Previous reports have shown, e.g., that the morphology of ZnO nanostructures is very dependent on the presence of In impurities in the growth system.[14] Impurities may in principle have two effects on the CTR-VPT growth,

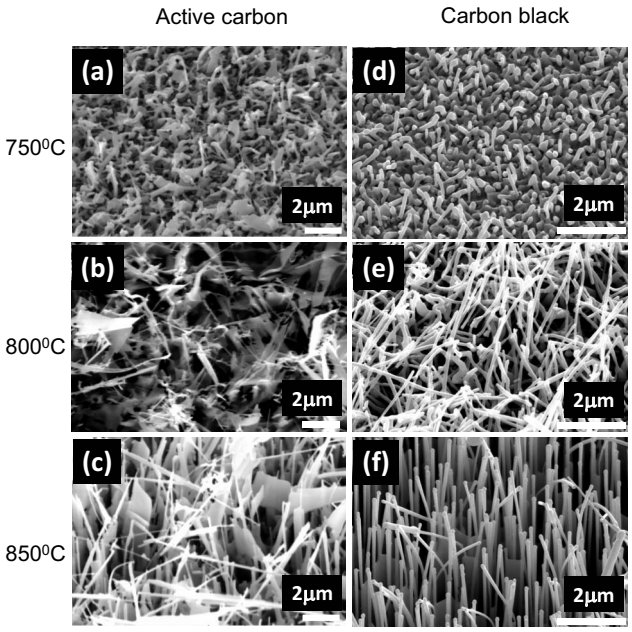

FIG. 4. FESEM images of samples grown using activated carbon at (a) 750 °C, (b) 800 °C, and (c) 850 °C and using carbon black at (d) 750 °C, (e) 800 °C, (f) 850 °C (using a carbon powder mass of 0.06 g in both cases).

firstly enabling Zn vapor production at lower temperatures which may occur either by direct ZnO reduction—common impurities such as Al, Si, Li, and Mg will all tend to reduce ZnO (Ref. 19) or by catalysis of the CTR reaction, thus potentially increasing yields at lower growth temperatures. Secondly, impurities in the gas stream may affect the deposit morphology via alteration of surface energies of various ZnO facets, as shown by Fan *et al.* for In contamination.[14] However, CTR-VPT growth in our system using two much lower purity graphites with a range of metal and other impurities [(i) Sigma-Aldrich-Fluka; 99% purity graphite powder with 11.2 m^2/g surface area, (ii) Alfa Aesar; 99.9% purity graphite flake with 1.6 m^2/g surface area] show identical results both in terms of yield and morphology to Figs. 1 and 3 above, i.e., well-aligned nanorods at 850 °C, almost no deposit at 750 °C and the beginnings of nanorod nucleation at 800 °C (data not shown). Thus we do not believe that impurities in the carbon are singularly responsible for the effects we observe. We note also that chemical analyses provided by the suppliers using inductively coupled plasma optical emission spectroscopy (ICP-OES) and our own energy dispersive x-ray (EDX) analyses of a selection of the carbon powders used in this work showed no evidence of In contamination, down to a detection limit of ppm using ICP-OES and of ~0.1% concentration using EDX.

We interpret our data to mean that the differences in growth we see are associated with the high surface activity of nongraphite carbon sources which is related to, but not completely determined by surface area, as discussed previously.[13] Surface activity originates both at edges and defects of the carbon layers and at the locations of heteroatoms such as oxygen, hydrogen, sulfur, and nitrogen which introduce active sites on the carbon surface, and surface activity is known to play a crucial role in the surface chemistry of the many carbon materials.[13,23] We note that the involvement of heteroatoms in the surface activity might be described as an impurity effect, which we have discussed above; however, the key point is that the presence of impurities alone is not the origin of the effects, but rather the specific binding to the carbon layers of such heteroatoms during the carbon synthesis which creates active carbon sites (in addition to intrinsic effects such as edges and defects of the carbon layers), thus enabling the CTR. The surface activity of carbon blacks may equal or exceed that of active carbons, despite the lower surface areas for the carbon blacks, especially for untreated active carbons, which is the type we have used.[13,24] This conclusion is consistent with our data and also with the other reported data in literature since the surface activity of carbon blacks generally is quite high and will also be appreciable for other carbon species such as SWNT and MWNT where layer defects and edges are expected to be important.[8,9,16,25] However, the surface activity of such powders is also a rather variable quantity and is crucially dependent on the material preparation and processing conditions so that variations from report to report in terms of the details of yield and morphology are expected due to the different sources of the carbon powders used.[13]

The effects of higher surface activity of nongraphite carbons on the nanostructure yield are easily understood since the higher surface activity will enable the CTR reaction to proceed at much lower temperatures due to the availability of a suitable quantity of reactive carbon atoms/active sites and thus enable appreciable nanostructure yields at lower temperatures. The issue of why different nanostructure morphologies are observed using nongraphite carbons is less easily understood. Our studies with lower purity graphites indicate that impurities in the carbon source are not the singular origin of the differences in morphology in our experiments (unlike the results in Ref. 14 for In contamination). At the present stage of our investigations, we are examining firstly whether the differences in morphology may be due either to the effects of higher Zn pressures on the nanostructure nucleation and growth mechanisms. Secondly, the active sites, which are the source of the CTR reaction in carbon blacks in many cases, are the sites of heteroatom binding, which is, in turn, the cause of the local surface activity. The CTR reaction, which occurs in the vicinity of such heteroatoms, may lead to the release of the heteroatoms or complexes containing heteroatoms into the Zn vapor stream which ultimately condenses at the substrate to form nanostructures. The presence of the heteroatoms in the condensing vapor stream may also lead to changes in the nanostructure morphology. These aspects related to the varying nanostructure morphology are the subject of an ongoing study.

CONCLUSIONS

In conclusion, our data show that the different deposit yields and morphologies observed in CTR-VPT growth of ZnO nanostructures using different carbon powders cannot be explained by surface area, thermodynamic effects, or purity differences alone. Rather, the differing surface activities

of the carbon powders are responsible in our experiments. The use of different types of carbon powders does enable growth at significantly lower temperatures and with different morphologies, including smaller nanowire diameters in certain temperature regions, which may be useful for applications in, e.g., field emission.[26] However, the negative side of this achievable diversity is that reproducible deposit yields and morphologies are more difficult to achieve with carbon powders whose chemical properties, and specifically, surface activities are more variable. Clearly there is a trade-off between the relative advantages that lower temperature growth using nongraphite powders may offer in terms of nanostructure diversity and range of available substrates and the drive to develop industrial scale uses of ZnO nanostructures for which reproducibility and scalability are key considerations. For the latter applications, the use of graphite powder may be preferred, since, based on our data, the surface chemistry/activity of graphite powders appears quite reproducible for graphite from various sources and with varying purities and SSA.

Note added in proof: Recent experiments at higher temperatures above the crossing points on the Ellingham diagram of the $2Zn+O_2 \rightarrow 2ZnO$ line with the $2C+O_2 \rightarrow 2CO$ line ($>950\,^{\circ}C$) indicate that Gibbs free energy effects may lead to differences in deposit quantity for samples grown using carbon black compared to those grown with activated carbon when the CTR reaction has a negative free energy change and is strongly favoured. However, at the temperatures used for the samples considered here, below the crossing points, such effects do not explain our results.

ACKNOWLEDGMENTS

The authors acknowledge financial support from an SFI-RFP grant (No. 06/RFP/PHY052). We gratefully acknowledge the assistance of Ms. Veronica Dobbyn (School of Chemical Sciences, Dublin City University) who made measurements of the purity levels of various carbon powders. We further thank Professor Francisco Rodríguez Reinoso (Universidad de Alicante), Dr. Peter J. F. Harris (University of Reading), and Dr. Tommy Yang and colleagues (Micromeritics) for their valuable assistance in answering email queries related to this work.

[1] Z. L. Wang, J. Phys.: Condens. Matter **16**, R829 (2004).
[2] Z. L. Wang, Mater. Today **7**, 26 (2004).
[3] P. D. Yang, H. Yan, S. Mao, R. Russo, J. Johnson, R. Saykally, N. Morris, J. Pham, R. He, and H.-J. Choi, Adv. Funct. Mater. **12**, 323 (2002).
[4] M. H. Huang, Y. Y. Wu, H. Feick, N. Tran, E. Weber, and P. D. Yang, Adv. Mater. (Weinheim, Ger.) **13**, 113 (2001).
[5] P. W. Atkins, *Physical Chemistry*, 5th ed. (Oxford University Press, Oxford, 1994).
[6] C. G. Maier, U.S. Bureau of Mines, Bulletin No. 324, 1930.
[7] J.-R. Duclère, B. Doggett, M. O. Henry, E. McGlynn, R. T. Rajendra Kumar, J.-P. Mosnier, A. Perrin, and M. Guilloux-Viry, J. Appl. Phys. **101**, 013509 (2007).
[8] Y. S. Lim, J. W. Park, M. S. Kim, and J. Kim, Appl. Surf. Sci. **253**, 1601 (2006).
[9] Y. H. Leung, A. B. Djurisic, J. Gao, M. H. Xie, Z. F. Wei, S. J. Xu, and W. K. Chan, Chem. Phys. Lett. **394**, 452 (2004).
[10] G. Gundiah, F. L. Deepak, A. Govindaraj, and C. N. R. Rao, Top. Catal. **24**, 137 (2003).
[11] Y. Hang Leung, A. B. Djurisic, J. Gao, M. H. Xie, and W. K. Chan, Chem. Phys. Lett. **385**, 155 (2004).
[12] M. Biswas, E. McGlynn, and M. O. Henry, Microelectron. J. **40**, 259 (2009).
[13] F. Rodríguez-Reinoso, Carbon **36**, 159 (1998) and references therein.
[14] H. J. Fan, A. S. Barnard, and M. Zacharias, Appl. Phys. Lett. **90**, 143116 (2007).
[15] JCPDS Card No. 36-1451 (for ZnO); JCPDS Card No. 46-1212 (for Al_2O_3).
[16] Y. S. Lim, J. W. Park, S. T. Hong, and J. Kim, Mater. Sci. Eng., B **129**, 100 (2006).
[17] P. J. F. Harris, Crit. Rev. Solid State Mater. Sci. **30**, 235 (2005).
[18] J.-B. Donnet, Carbon **32**, 1305 (1994).
[19] Glushko Thermocenter of the Russian Academy of Sciences in the IVTANTHERMO database and listed at; http://www.chem.msu.su/rus/tsiv/Zn/table.Zn.6.html.
[20] B. S. Terry and X. Yu, Ironmaking Steelmaking **18**, 27 (1991).
[21] J. S. Speck, J. Appl. Phys. **67**, 495 (1989).
[22] S. K. Das and E. E. Hucke, Carbon **13**, 33 (1975).
[23] C. Poleunis, X. Vanden Eynde, E. Grivei, H. Smet, N. Probst, and P. Bertrand, Surf. Interface Anal. **30**, 420 (2000).
[24] A. Schroeder, M. Klueppel, and R. H. Schuster, Macromol. Mater. Eng. **292**, 885 (2007).
[25] S. Banerjee, T. Hemraj-Benny, and S. S. Wong, Adv. Mater. (Weinheim, Ger.) **17**, 17 (2005).
[26] R. T. Rajendra Kumar, E. McGlynn, C. McLoughlin, S. Chakrabarti, R. C. Smith, J. D. Carey, J. P. Mosnier, and M. O. Henry, Nanotechnology **18**, 215704 (2007).